

Diversity of Vegetation Patterns and Desertification

J. von Hardenberg,^{1,4} E. Meron,^{1,3} M. Shachak,² and Y. Zarmi^{1,3}

¹Department of Solar Energy and Environmental Physics, BIDR, Ben Gurion University, Sede Boker Campus 84990, Israel

²Mitrani Department of Desert Ecology, BIDR, Ben Gurion University, Sede Boker Campus 84990, Israel

³Department of Physics, Ben Gurion University, Beer Sheva 84105, Israel

⁴Institute for Scientific Interchange, Viale Settimio Severo 65, 10133 Torino, Italy

(Received 29 May 2001; published 18 October 2001)

A new model for vegetation patterns is introduced. The model reproduces a wide range of patterns observed in water-limited regions, including drifting bands, spots, and labyrinths. It predicts transitions from bare soil at low precipitation to homogeneous vegetation at high precipitation, through intermediate states of spot, stripe, and hole patterns. It also predicts wide precipitation ranges where different stable states coexist. Using these predictions we propose a novel explanation of desertification phenomena and a new approach to classifying aridity.

DOI: 10.1103/PhysRevLett.87.198101

PACS numbers: 87.23.Cc, 89.75.Kd

Vegetation patches, a subfield of spatial ecology [1,2], have been extensively studied by arid land ecologists [3]. The dominating driving forces in arid lands are water scarcity, plant competition over water resources, and redistribution of water by runoff. A widespread example is vegetation bands on hill slopes [4], shown in Fig. 1a. The formation of bands is a result of low water infiltration in bare soil compared to vegetated soil, and the consequent accumulation of runoff at vegetation patches.

The view of vegetation patches as a pattern formation phenomenon involving symmetry breaking is fairly new. This view is supported by recent mathematical models that identify vegetation patterns with instabilities of uniform vegetation states [5–10]. The models account for field observations of various vegetation patterns including bands on hill slopes and spots in plain areas. No attempt, however, has been made to use such vegetation models to investigate questions of broader ecological context such as desertification.

In this Letter, we introduce a new model for vegetation dynamics that involves two variables, the plant biomass and the water available to the plants. The main new ingredient in this model is the introduction of a term that simulates the competition of vegetation patches for water due to water uptake by roots. The model reproduces a wide range of patterns observed in arid and semiarid regions, including forms that have not been explained yet, such as rings. Using this model, we study sequences of vegetation states, as a precipitation parameter is increased, and identify precipitation ranges where different stable states coexist. The outcomes of this study are used to propose a theoretical explanation of desertification phenomena in terms of hysteresis loops, and to propose a new classification of aridity based on the inherent vegetation states of the system. These results shed light on questions such as the vulnerability of drylands to desertification, the irreversibility of desertification, and the prospects of human intervention in recovering bioproductivity.

We propose the following model for the biomass density $n(\mathbf{x}, t)$ and the ground water density $w(\mathbf{x}, t)$:

$$\frac{\partial n}{\partial t} = \frac{\gamma w}{1 + \sigma w} n - n^2 - \mu n + \nabla^2 n, \quad (1)$$

$$\frac{\partial w}{\partial t} = p - (1 - \rho n)w - w^2 n + \delta \nabla^2 (w - \beta n) - v \frac{\partial (w - \alpha n)}{\partial x}, \quad (2)$$

where all quantities are in nondimensional form. The term $\frac{\gamma w}{1 + \sigma w} n$ in Eq. (1) describes plant growth at a rate that grows linearly with w for dry soil. The term $-\mu n$ accounts for mortality and herbivory, and the quadratic term $-n^2$

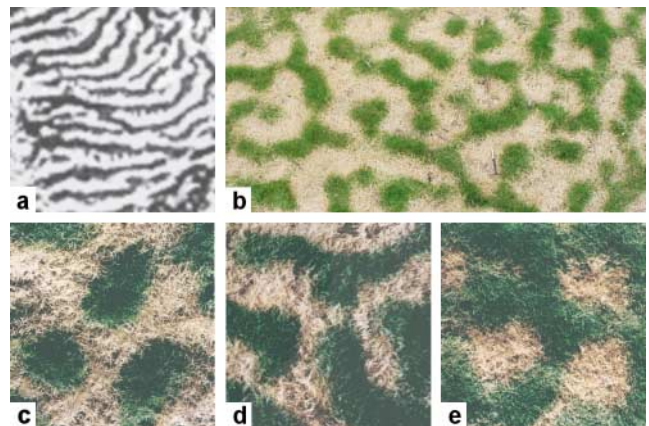


FIG. 1 (color). Field observations of vegetation patterns. Bands (a) on hill slopes in Niger. Band width is in the range of a few tens of meters. Reprinted from *Catena*, Ref. [4], ©1999, with permission from Elsevier Science. A labyrinth (b), spots (c), stripes (d), and holes (e) of green biomass of the perennial grass *Paspalum vaginatum*, observed in a residential neighborhood in the northern Negev (200 mm mean annual rainfall). The distance between spots/stripes is of the order of 15 cm.

represents saturation due to limited nutrients. The spread of plants, both by clonal reproduction and by seed dispersal is modeled by the diffusion term $\nabla^2 n$ [11].

Equation (2) contains a source term p representing precipitation, and a loss term $-(1 - \rho n)w$ representing evaporation. Vegetation reduces evaporation ($\rho > 0$) by shading and increased infiltration due to soil accumulation and absence of microbial crusts [12]. Local uptake of water by plants (mostly transpiration) is modeled by the term $-w^2 n$ (this form was motivated by transpiration curves appearing in Ref. [13]). The transport of water in the soil is modeled by Darcy's law which states that the water flux \mathbf{J} is proportional to the gradient of the water matric potential ϕ [13]. To account for the suction of water by the roots we assume the form $\phi = \phi_0 - \beta n$, where ϕ_0 is the matric potential for bare soil, and we use the simple form $\phi_0 = w$, assuming constant hydraulic diffusivity [13]. The temporal change of w due to transport, $-\nabla \cdot \mathbf{J} \propto \nabla^2 \phi$, gives the Laplacian term in Eq. (2). Surface runoff is modeled by the term $-v \frac{\partial h}{\partial x}$, where v is a constant downhill runoff flow velocity and $h(\mathbf{x}, t)$ is the runoff height, which in the absence of vegetation we take to be proportional to w . To model the drop of runoff in vegetated areas due to increased infiltration, we assume the form $h = w - \alpha n$. The water dependent, plant-growth term in Eq. (1) and the terms containing the parameters ρ , β , and α in Eq. (2) describe *positive feedback* effects of water and biomass [14]. Realistic values for the parameters in Eqs. (1) and (2) have been determined following Refs. [13,15].

We study this model by performing a stability analysis of uniform solutions and integrating Eqs. (1) and (2) numerically at different precipitation values p . The results for a plain landscape (excluding runoff) are summarized in Fig. 2, which shows the spatially averaged biomass $\langle n \rangle$ as a function of p . The model has a uniform bare state (no vegetation) for all constant p values. This state is represented by the solution $n = 0, w = p$, shown in Fig. 2 as the horizontal line \mathcal{B} . The bare state is stable (solid line) at precipitation values lower than a critical value p_c . Above this threshold the bare state becomes unstable (dashed line) and a new state appears, shown in Fig. 2 as line \mathcal{V} . This state represents a uniformly distributed vegetation with biomass density monotonically increasing with p . It is stable only for relatively low precipitation values, $p_c < p < p_1$ and it regains stability at high precipitation values, $p > p_2$, where the biomass density is high. (The thresholds p_c , p_1 , and p_2 can be derived analytically.)

In the intermediate precipitation range, $p_1 < p < p_2$, uniform vegetation is unstable to finite wave number perturbations [11,16], which evolve into vegetation patterns of various forms as shown in the insets in Fig. 2. This instability is caused by the competition of vegetation patches over water resources [modeled by the Laplacian term in Eq. (2)]. The type of pattern depends on the precipita-

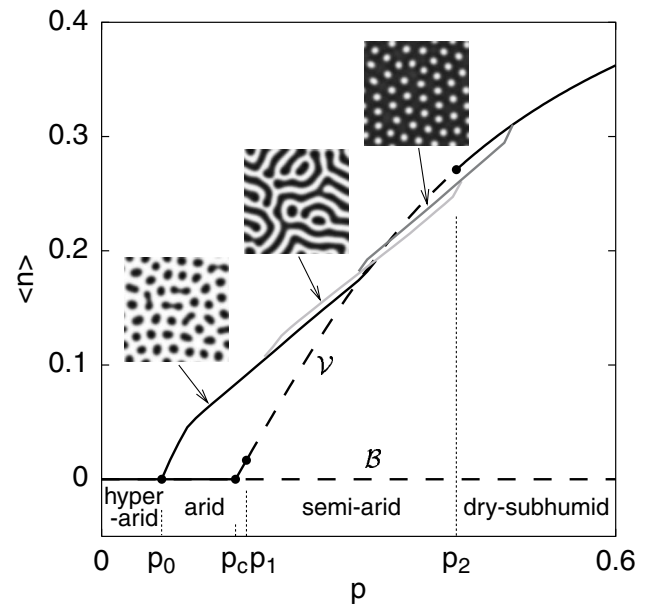


FIG. 2. Spatially averaged biomass $\langle n \rangle$ vs precipitation p for plain landscape ($v = 0$). The line \mathcal{B} represents the bare state $\langle n \rangle = 0$. The curved line \mathcal{V} designates the uniform vegetation state. The insets show typical patterns associated with the different nonuniform solution branches denoted by the black and gray lines. Parameter values used are $\gamma = 1.6$, $\sigma = 1.6$, $\mu = 0.2$, $\rho = 1.5$, $\delta = 100$, $\alpha = 3$, and $\beta = 3$. For these parameters and with realistic scalings $p = 1$ corresponds to 800 mm annual rainfall, and $n = 1$ to 1.25 kg/m² of biomass density.

tion range: vegetation spots at relatively low p , stripes (or labyrinths) at intermediate p , and holes in a uniform coverage at relatively high p values. These patterns reflect optimal self-organization of the system with respect to water resources. Spot patterns are the preferred patterns at low p since water uptake from adjacent bare areas can be made in all directions. Stripes, which have only two directions to extract water from, need higher precipitation values [17].

Including runoff in Eq. (2) ($v \neq 0$) simulates the effects of hill slopes. As Fig. 3 shows, bands of vegetation drifting uphill become the preferred pattern for a wide range of precipitation. As the precipitation decreases “dashed” patterns develop.

Most of the patterns discussed above have been observed in the field. Spotted, dashed, and banded patterns have been found in a wide range of geographical areas throughout the world [4]. The same patterns have been observed on different length scales with different species. Very often the patterns involve more than one species. Figure 1a shows field observations of banded patterns on hill slopes in Niger. The bands are oriented perpendicular to the slope direction. The effects of rainfall and slope on vegetation patterns implied by Figs. 2 and 3 are consistent with field observations [4]. Figure 1b shows an observation of a labyrinthine pattern of the perennial grass *Paspalum vaginatum*. Figures 1c–1e show closeups at different

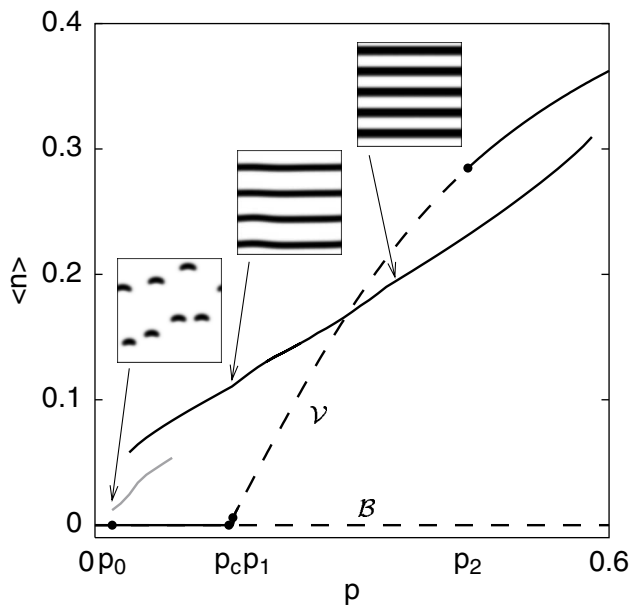


FIG. 3. Spatially averaged biomass $\langle n \rangle$ vs precipitation p on a slope, $\nu = 30$. The lines \mathcal{B} and \mathcal{V} represent uniform bare and uniform vegetation states, respectively. The insets show typical banded and dashed patterns associated with the nonuniform solution branches (black and gray lines, respectively). Parameter values other than ν are as in Fig. 2.

locations of the same area that reveal the three pattern states (compare with the insets in Fig. 2) [18].

Transients toward asymptotic patterns may involve additional forms. Spots growing into rings due to the strong competition for water at the spots' centers is one example. Simulations of ring formation as well as field observations will be reported elsewhere.

Figure 2 indicates the possible coexistence of different stable states under the same rainfall conditions. The coexistence is a result of the positive feedback between biomass and water. Consider, for example, the precipitation range $p_0 < p < p_c$ where a stable spot pattern coexists with a stable bare soil (see Fig. 2). Vegetation spots having well-developed root systems, are effective in extracting water from their bare surroundings and therefore survive. On the other hand, low biomass perturbations of the bare state have poor water uptake capabilities and die out, leaving the bare state stable. As a result, the two states can stably coexist at the same precipitation value. The coexistence of states may also involve different patterns. In that case the differences in biomass might be small but other, nonwater related ecological characteristics may differ significantly due to the different connectivity of the patterns.

The coexistence of stable states suggests a new view of *desertification*, a land degradation phenomenon of high concern today [19]. Desertification involves a decrease in biological productivity due to climatic changes (like drought) or human activities (like overgrazing), and leads to a long lasting and possibly irreversible degraded state

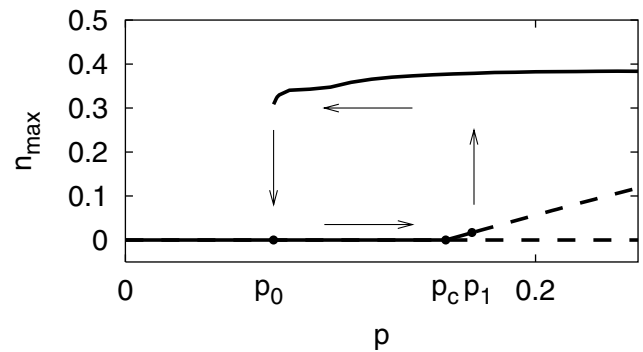


FIG. 4. Biomass amplitude n_{\max} in the low precipitation regime. The figure illustrates the view of desertification as a hysteretic loop.

[20]. These two elements naturally emerge in our model as transitions between coexisting states. Two scenarios of such transitions can be distinguished: transitions induced by precipitation changes (hysteresis), describing desertification due to climatic causes, and transitions induced by biomass perturbations, describing desertification due to human activities.

Figure 4 illustrates the first scenario, desertification due to climatic changes. It shows an enlargement of the low precipitation range in Fig. 2 except that the vertical axis represents the biomass amplitude rather than the average. Imagine the system is initially in the spot-pattern state. A drought period shifts the system along the pattern branch toward lower biomass values. A prolonged drought may drive the system beyond the edge of the pattern branch, down to the bare state (see down arrow). A rainy season that follows the drought and brings back the precipitation level to its original value *may not* recover the spots state, due to the inability of low biomass vegetation to effectively extract water from the bare surroundings. Considerably higher precipitation values may be needed to close the hysteresis loop (see up arrow) and recover the original spots state of the system. The range of coexistence of the pattern and bare states determines the size of the hysteresis loop and, consequently, the extent of irreversibility of the associated desertification process.

The second scenario, desertification due to human activities, is related to the unstable pattern state that exists between the bare state and the spot-pattern state in their range of coexistence. This state defines a threshold biomass distribution [21]. A perturbation of the spot-pattern state below the threshold will lead to a recovery of the biomass. A perturbation that exceeds the threshold (e.g., *overgrazing*), will induce a transition to the bare state or desertification.

The two scenarios of desertification apply to other ranges of precipitation, where two different stable states coexist, such as uniform coverage and holes, holes and stripes, stripes and spots.

The changes of the system's states along a rainfall gradient shown in Fig. 2 suggest a new approach to the

classification of aridity. The term *aridity* refers to a permanent pluviometric deficit whose strength bears on the degree of vegetation the system can support. Aridity classes are introduced to reflect different vegetation states at different pluviometric conditions, defined by the annual rain fall or the aridity index (ratio of annual rainfall to potential evapotranspiration rate) [22]. The difficulty with this approach lies in the choice of the threshold values of the aridity index that distinguish between different classes. These thresholds do not take into account non-pluvial parameters that affect the vegetation states of the system, like topography. To circumvent this difficulty we propose to use the *inherent vegetation states* of the system as a basis for classifying aridity. A possible classification is as follows:

Dry-subhumid.—The only stable states the system supports correspond to uniform vegetation or vegetation patterns ($p > p_2$ in Fig. 2).

Semiarid.—The system does not support uniform vegetation nor a bare soil. The only possible stable states correspond to vegetation patterns ($p_1 < p < p_2$).

Arid.—The only stable states the system supports correspond to bare soil, “grass” (low amplitude uniform vegetation), or vegetation patterns ($p_0 < p < p_1$).

Hyperarid.—The only stable state the system supports is bare soil ($p < p_0$).

Note that the thresholds p_0, p_1, p_2 define now sharp transitions between different vegetation states. Vegetation *cannot* exist in a hyperarid zone ($p < p_0$), for example, while it may exist in an arid zone ($p_0 < p < p_1$). Unlike classifications in current use, the thresholds p_0, p_1, p_2 , are not numerical constants, but rather functions of nonpluvial parameters such as hill slope. Figures 2 and 3 illustrate this dependence. The value of p_0 in the case of a hilly landscape (Fig. 3) is smaller than the corresponding one for a plain landscape (Fig. 2). The down shift of p_0 due to topography reflects the effect of water runoff and accumulation which allows for local vegetation in a precipitation range that does not support vegetation on flat landscapes.

Another advantage of the proposed classification pertains to the information it contains about dynamical aspects of drylands. Regions whose aridity classes imply coexistence of stable states are vulnerable to desertification as Fig. 4 shows. At the same time these regions lend themselves to recovery operations by human intervention such as crust disturbance and seed augmentation.

The implementation of the proposed classification requires long term observations of the diversity, the coexistence, and the time evolution of vegetation patterns. Small-scale experimentation may also be needed in ambiguous situations where the aridity class cannot be inferred from the observed land coverage.

We presented here a new mathematical model that accounts for a wide range of vegetation patterns observed in drylands. Using this model we demonstrated the potential advantage of a dynamical systems approach in the study of

dryland ecosystems. The coexistence of stable states sheds new light on desertification phenomena. The sequence of stable states along a rainfall gradient motivates a classification of aridity that better reflects system properties such as vulnerability to desertification.

J. H. acknowledges support by the European LSF programme and by BCSC at BIDR.

-
- [1] *Modeling Spatiotemporal Dynamics in Ecology*, edited by J. Bascompte and R. V. Sole (Springer-Verlag, Berlin, 1998).
 - [2] *Spatial Ecology*, edited by D. Tilman and P. Kareiva (Princeton University Press, Princeton, 1997).
 - [3] M. R. Aguiar and O. E. Sala, *TREE* **14**, 273 (1999).
 - [4] C. Valentin and J. M. d’Herbès, and J. Poesen, *Catena* **37**, 1 (1999).
 - [5] C. A. Klausmeier, *Science* **284**, 1826 (1999).
 - [6] R. HilleRisLambers, M. Rietkerk, F. van den Bosch, H. H. T. Prins, and H. de Kroon, *Ecology* **82**, 50 (2001).
 - [7] J. Thiéry, J. M. d’Herbès, and C. Valentin, *J. Ecol.* **83**, 497 (1995).
 - [8] R. Lefever and O. Lejeune, *Bull. Math. Biol.* **59**, 263 (1997).
 - [9] O. Lejeune and M. Tlidi, *J. Veg. Sci.* **10**, 201 (1999).
 - [10] R. Lefever, O. Lejeune, and P. Couteron, in *Mathematical Models for Biological Pattern Formation, IMA*, edited by P. K. Maini and H. Othmer (Springer, New York, 2000), Vol. 121, p. 83.
 - [11] J. D. Murray, *Mathematical Biology* (Springer-Verlag, Berlin, 1989).
 - [12] N. E. West, *Adv. Ecol. Res.* **20**, 179 (1990).
 - [13] D. Hillel, *Environmental Soil Physics* (Academic Press, San Diego, 1998).
 - [14] J. B. Wilson and A. D. Q. Agnew, *Adv. Ecol. Res.* **23**, 263 (1992).
 - [15] O. L. Lange and P. S. Nobel, in *Physiological Plant Ecology II*, edited by C. B. Osmond and H. Ziegler (Springer-Verlag, Berlin, 1982).
 - [16] M. C. Cross and P. C. Hohenberg, *Rev. Mod. Phys.* **65**, 851 (1993).
 - [17] The sequence of states, bare, spots (“0-hexagons”), stripes, holes (“ π -hexagons”), and uniformly vegetated, was also found in a single-variable vegetation model as an aridity parameter was varied [8–10].
 - [18] The sequence spots-stripes-holes of *P. vaginatum* has been observed in the same park in one occasion, suggesting coexistence of all the three pattern states, although sunlight exposure was not uniform. Coexistence of the three states is produced by the model in a narrow precipitation range (see Fig. 2).
 - [19] United Nations Convention to Combat Desertification, <http://www.unccd.int/main.php>
 - [20] U. Helld’n, *Desertification Control Bull.* **17**, 8 (1988).
 - [21] The threshold biomass distribution cannot be calculated by the numerical method used here (a PDE solver). We postpone this calculation to a sequel study.
 - [22] M. Mainguet, *Aridity: Droughts and Human Development* (Springer-Verlag, Berlin, 1999).